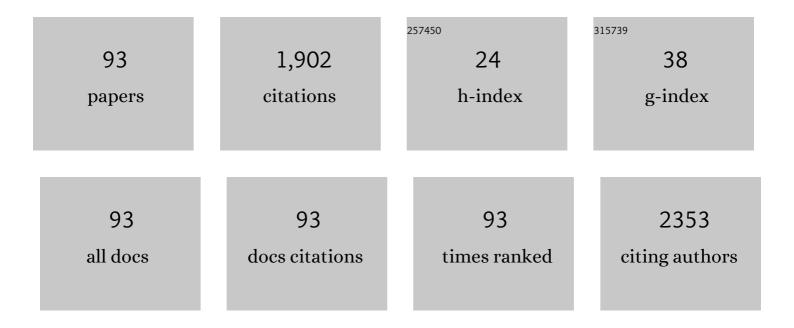
List of Publications by Year in descending order

Source: https://exaly.com/author-pdf/7321392/publications.pdf Version: 2024-02-01



#	Article	IF	CITATIONS
1	Flexible rGO-SnO2 supercapacitors converted from pastes containing SnCl2 liquid precursor using atmospheric-pressure plasma jet. Ceramics International, 2021, 47, 1651-1659.	4.8	13
2	Atmospheric pressure plasma jet fabricating of porous silver electrocatalyst as a promising approach to the creation of cathode layers of low temperature solid oxide fuel cells. Surface and Coatings Technology, 2021, 410, 126810.	4.8	6
3	Carbon Dioxide Tornado-Type Atmospheric-Pressure-Plasma-Jet-Processed rGO-SnO2 Nanocomposites for Symmetric Supercapacitors. Materials, 2021, 14, 2777.	2.9	9
4	Atmospheric Pressure Tornado Plasma Jet of Polydopamine Coating on Graphite Felt for Improving Electrochemical Performance in Vanadium Redox Flow Batteries. Catalysts, 2021, 11, 627.	3.5	4
5	A Facile Nitriding Approach for Improved Impact Wear of Martensitic Cold-Work Steel Using H2/N2 Mixture Gas in an AC Pulsed Atmospheric Plasma Jet. Coatings, 2021, 11, 1119.	2.6	4
6	Metal-Organic Frameworks Derived Catalyst for High-Performance Vanadium Redox Flow Batteries. Catalysts, 2021, 11, 1188.	3.5	4
7	Achieving Selective Cleaning on Semiconductors Packaging Using Atmospheric Pressure Plasma. , 2020, , .		0
8	Wettability, electron work function and corrosion behavior of CoCrFeMnNi high entropy alloy films. Surface and Coatings Technology, 2020, 400, 126222.	4.8	27
9	Editorial: The biennial TACT international thin films conference (TACT 2019). Thin Solid Films, 2020, 709, 138210.	1.8	0
10	Tailoring surface properties of polyethylene terephthalate by atmospheric pressure plasma jet for grafting biomaterials. Thin Solid Films, 2020, 709, 138152.	1.8	14
11	Formation of Aluminum Composite Passive Film on Magnesium Alloy by Integrating Sputtering and Anodic Aluminum Oxidation Processes. Thin Solid Films, 2020, 709, 138151.	1.8	16
12	Effects of cyclonic plasma deposited organosilicon nano oating on 316 stainless steel and its surface characterization. Surface and Interface Analysis, 2019, 51, 993-1000.	1.8	8
13	Improving the Solder Wettability Via Atmospheric Plasma Technology. , 2019, , .		5
14	Dual RGD-immobilized poly(L-lactic acid) by atmospheric pressure plasma jet for bone tissue engineering. Colloids and Surfaces B: Biointerfaces, 2019, 178, 358-364.	5.0	11
15	Functional FAS-13/SiOx composite coatings for improved anticorrosion and hydrophobicity/oleophobicity on AZ91D magnesium alloys. Japanese Journal of Applied Physics, 2019, 58, SAAD03.	1.5	3
16	Fluoride at waste oyster shell surfaces – Role of magnesium. Science of the Total Environment, 2019, 652, 1331-1338.	8.0	31
17	Fabrication of in operando, self-growing, core-shell solid electrolyte interphase on LiFePO4 electrodes for preventing undesirable high-temperature effects in Li-ion batteries. Electrochimica Acta, 2018, 268, 260-267.	5.2	7
18	The enhanced abrasion resistance of an anti-fingerprint coating on chrome-plated brass substrate by integrating sputtering and atmospheric pressure plasma jet technologies. Applied Surface Science, 2018, 448, 88-94.	6.1	12

Үи-Lім Кио

#	Article	IF	CITATIONS
19	Tailoring the O2 reduction activity on hydrangea-like La0.5Sr0.5MnO3 cathode film fabricated via atmospheric pressure plasma jet process. Ceramics International, 2018, 44, 7349-7356.	4.8	13
20	Transparent sapphire substrates with tunable optical properties by decorating with nanometric oxide on porous anodic aluminum oxide patterns. Ceramics International, 2018, 44, 10898-10906.	4.8	4
21	Redox performance of Na-modified Fe2O3/Al2O3 with syngas as reducing agent in chemical looping combustion process. Chemical Engineering Journal, 2018, 334, 2079-2087.	12.7	40
22	Electric arc furnace dust as an alternative low-cost oxygen carrier for chemical looping combustion. Journal of Hazardous Materials, 2018, 342, 297-305.	12.4	20
23	Oxygen vacancy levels on gadolinia-doped ceria interlayer deposited by atmospheric pressure plasma jet for solid oxide fuel cells. Ceramics International, 2018, 44, 15262-15268.	4.8	8
24	Microwave effect on barium strontium ferrate and co-fired fuel cells. International Journal of Hydrogen Energy, 2018, 43, 13393-13405.	7.1	0
25	In operando measurements of kinetics of solid electrolyte interphase formation in lithium-ion batteries. Journal of Power Sources, 2018, 400, 426-433.	7.8	9
26	Improvement of photocatalytic activities of Ag/P25 hybrid systems by controlled morphology of Ag nanoprisms. Materials Chemistry and Physics, 2017, 192, 78-85.	4.0	14
27	A facile method for sodium-modified Fe 2 O 3 /Al 2 O 3 oxygen carrier by an air atmospheric pressure plasma jet for chemical looping combustion process. Chemical Engineering Journal, 2017, 316, 15-23.	12.7	20
28	Liquid sintering behavior of Cu-based oxygen carriers for chemical looping process. Catalysis Communications, 2017, 92, 70-74.	3.3	13
29	Mechanism of oxygen ion diffusion in Gd-doped ceria electrolyte films deposited via reactive and direct sputtering. Surface and Coatings Technology, 2017, 320, 47-52.	4.8	7
30	Electrocatalysis enhancement of a screenâ€printed carbon electrode by modification with trisoctahedral gold nanocrystals for H ₂ O ₂ and <scp>NADH</scp> sensing application. Journal of Chemical Technology and Biotechnology, 2017, 92, 2460-2467.	3.2	2
31	Utilization of electric arc furnace dust as regenerable sorbents for the removal of hydrogen sulfide. Ceramics International, 2017, 43, S694-S699.	4.8	13
32	Carbon-free SiOx ultrathin film using atmospheric pressure plasma jet for enhancing the corrosion resistance of magnesium alloys. Vacuum, 2017, 146, 8-10.	3.5	12
33	Fabrication of Fe2O3/TiO2 Oxygen Carriers for Chemical Looping Combustion and Hydrogen Generation. Aerosol and Air Quality Research, 2016, 16, 2023-2032.	2.1	7
34	Sputter-deposited 20 mol% gadolinia-doped ceria films on 8 mol% yttria-stabilized zirconia tapes for improved electrochemical performance. Thin Solid Films, 2016, 618, 202-206.	1.8	4
35	Ascorbic Acidâ€Assisted Synthesis of Mesoporous Sodium Vanadium Phosphate Nanoparticles with Highly sp ² oordinated Carbon Coatings as Efficient Cathode Materials for Rechargeable Sodiumâ€ion Batteries. Chemistry - A European Journal, 2016, 22, 10620-10626.	3.3	55
36	Optimization of Mechanical Properties of UV-cut Polyester Fiber Using a Hybrid Taguchi and Fuzzy Approach. Journal of Engineered Fibers and Fabrics, 2015, 10, 155892501501000.	1.0	2

#	Article	IF	CITATIONS
37	Alginate/Poly(<i>Ĵ³</i> -glutamic Acid) Base Biocompatible Gel for Bone Tissue Engineering. BioMed Research International, 2015, 2015, 1-7.	1.9	17
38	Effect of Surfactant and Budesonide on the Pulmonary Distribution of Fluorescent Dye in Mice. Pediatrics and Neonatology, 2015, 56, 19-24.	0.9	22
39	Study of Poly (3,4-ethylenedioxythiophene)/MnO2 as Composite Cathode Materials for Aluminum-Air Battery. Electrochimica Acta, 2015, 176, 1324-1331.	5.2	23
40	Rice husk as solid fuel for chemical looping combustion in an annular dual-tube moving bed reactor. Chemical Engineering Journal, 2015, 280, 82-89.	12.7	14
41	Adsorption and precipitation of fluoride on calcite nanoparticles: A spectroscopic study. Separation and Purification Technology, 2015, 150, 325-331.	7.9	64
42	Performance characterization of passive micromixer with dual opposing strips on microchannel walls. Chemical Engineering and Processing: Process Intensification, 2015, 93, 27-33.	3.6	10
43	A facile synthesis of high quality nanostructured CeO ₂ and Gd ₂ O ₃ -doped CeO ₂ solid electrolytes for improved electrochemical performance. Physical Chemistry Chemical Physics, 2015, 17, 14193-14200.	2.8	22
44	Atmospheric pressure plasma enhanced chemical vapor deposition of SiOx films for improved corrosion resistant properties of AZ31 magnesium alloys. Surface and Coatings Technology, 2015, 283, 194-200.	4.8	72
45	Use of Spinel Nickel Aluminium Ferrite as Self-Supported Oxygen Carrier for Chemical Looping Hydrogen Generation Process. Aerosol and Air Quality Research, 2015, 15, 2700-2708.	2.1	25
46	A facile method for the deposition of Gd2O3-doped ceria films by atmospheric pressure plasma jet. Thin Solid Films, 2014, 570, 215-220.	1.8	11
47	Preparation of composite nickel–iron oxide as highly reactive oxygen carrier for chemical-looping combustion process. Journal of the Taiwan Institute of Chemical Engineers, 2014, 45, 174-179.	5.3	18
48	Spent Isopropanol Solution as Possible Liquid Fuel for Moving Bed Reactor in Chemical Looping Combustion. Energy & Fuels, 2014, 28, 657-665.	5.1	12
49	Chemical looping combustion of polyurethane and polypropylene in an annular dual-tube moving bed reactor with iron-based oxygen carrier. Fuel, 2014, 135, 146-152.	6.4	16
50	One-step fabrication of tetragonal ZrO 2 particles by atmospheric pressure plasma jet. Powder Technology, 2014, 267, 74-79.	4.2	26
51	Mechanism of Fe2TiO5 as oxygen carrier for chemical looping process and evaluation for hydrogen generation. Ceramics International, 2014, 40, 4599-4605.	4.8	24
52	Methane combustion by moving bed fuel reactor with Fe2O3/Al2O3 oxygen carriers. Applied Energy, 2014, 113, 1909-1915.	10.1	51
53	Thermal stability, adhesion and electrical studies on (Ti,Zr)N x thin films as low resistive diffusion barriers between Cu and Si. Electronic Materials Letters, 2014, 10, 551-556.	2.2	4
54	Feasibility Study of Fe-ti based Oxygen Carriers for Chemical Looping Combustion. Energy Procedia, 2014, 61, 1398-1401.	1.8	1

Үи-Lім Кио

#	Article	IF	CITATIONS
55	Characterization and Evaluation of Prepared Fe2O3/Al2O3 Oxygen Carriers for Chemical Looping Process. Aerosol and Air Quality Research, 2014, 14, 981-990.	2.1	34
56	Assessment of redox behavior of nickel ferrite as oxygen carriers for chemical looping process. Ceramics International, 2013, 39, 5459-5465.	4.8	73
57	Effect of V2O5 doping on microstructure and electrical properties of Bi2O3–TiO2 solid oxide electrolyte system. Ceramics International, 2013, 39, 1711-1716.	4.8	7
58	Evaluation of the Photochemical Stability of Zinc Sulfide as Protective Layer on Silver Indium Sulfide Photocatalyst Film. Journal of the Chinese Chemical Society, 2012, 59, 1323-1328.	1.4	7
59	Assessment of thermochemically stable apatite La10(SiO4)6O3 as electrolyte for solid oxide fuel cells. Ceramics International, 2012, 38, 3955-3961.	4.8	25
60	Sintering behaviour and electrical properties of gadolinia-doped ceria modified by addition of silicon oxide and titanium oxide. Micro and Nano Letters, 2012, 7, 472.	1.3	10
61	Experimental analysis and optimization of the synthesizing property of nitrogenâ€modified TiO ₂ visibleâ€light photocatalysts. Journal of Chemical Technology and Biotechnology, 2012, 87, 160-164.	3.2	23
62	Preparation of platinum- and silver-incorporated TiO ₂ coatings in thin-film photoreactor for the photocatalytic decomposition of <i>o</i> -cresol. Environmental Technology (United Kingdom), 2011, 32, 1799-1806.	2.2	9
63	Assessment of structurally stable cubic Bi12TiO20 as intermediate temperature solid oxide fuels electrolyte. Journal of the European Ceramic Society, 2011, 31, 3119-3125.	5.7	12
64	Growth of 20mol% Gd-doped ceria thin films by RF reactive sputtering: The O2/Ar flow ratio effect. Journal of the European Ceramic Society, 2011, 31, 3127-3135.	5.7	15
65	Synthesis and study on phase diagram of 1–10mol% SnO2–doped Bi2O3. Journal of the European Ceramic Society, 2011, 31, 3153-3158.	5.7	8
66	Treatment of boron-containing optoelectronic wastewater by precipitation process. Desalination, 2011, 280, 146-151.	8.2	52
67	A study of parameter setting and characterization of visible-light driven nitrogen-modified commercial TiO2 photocatalysts. Journal of Hazardous Materials, 2011, 190, 938-944.	12.4	67
68	Material characteristics and electric properties of SiO <i>_x</i> -doped GDC electrolytes. Journal of the Chinese Institute of Engineers, Transactions of the Chinese Institute of Engineers,Series A/Chung-kuo Kung Ch'eng Hsuch K'an, 2011, 34, 31-38.	1.1	5
69	Mineralization of reactive Black 5 in aqueous solution by ozone/H2O2 in the presence of a magnetic catalyst. Journal of Hazardous Materials, 2010, 174, 795-800.	12.4	42
70	Characterization of electrolyte films deposited by using RF magnetron sputtering a 20mol% gadolinia-doped ceria target. Thin Solid Films, 2010, 518, 7229-7232.	1.8	16
71	Atmospheric-pressure plasma treatment on polystyrene for the photo-induced grafting polymerization of N-isopropylacrylamide. Thin Solid Films, 2010, 518, 7568-7573.	1.8	27
72	Superior Stability of Ultrathin and Nanocrystalline TiZrN Films as Diffusion Barriers for Cu Metallization. Nanoscience and Nanotechnology Letters, 2009, 1, 37-41.	0.4	5

#	Article	IF	CITATIONS
73	Reduction of free radicals and endotoxin by conjugated linoleic acid loaded in anin situ-synthesized poly(N-isopropyl acrylamide) thin layer. Journal of Applied Polymer Science, 2009, 113, 3222-3227.	2.6	4
74	Effects of Silver on the Photocatalytic Degradation of Gaseous Isopropanol. Water, Air, and Soil Pollution, 2009, 197, 313-321.	2.4	16
75	An electro-enhanced metalorganic chemical vapor deposition technique for producing thin copper films with (hfac)CuI(COD) as a precursor. Microelectronic Engineering, 2009, 86, 47-54.	2.4	2
76	Gadolinia-doped ceria films deposited by RF reactive magnetron sputtering. Solid State Ionics, 2009, 180, 1421-1428.	2.7	53
77	Reactions of Tp(NHî€CPh2)(PPh3)Ru–Cl with HCî€,CPh in the presence of H2O: insertion/hydration products. Dalton Transactions, 2009, , 4435.	3.3	24
78	Characteristics of Sputter-deposited Gadolinia-doped Ceria Thin Films on Al2O3/SiO2/Si Systems. Chinese Journal of Mechanical Engineering (English Edition), 2009, 22, 384.	3.7	1
79	Electroenhanced Metallorganic Chemical Vapor Deposition of Copper Films. Electrochemical and Solid-State Letters, 2007, 10, D51.	2.2	2
80	Effect of Pt/TiO2 characteristics on temporal behavior of o-cresol decomposition by visible light-induced photocatalysis. Water Research, 2007, 41, 2069-2078.	11.3	127
81	A DSC study on the kinetics of disproportionation reaction of (hfac)Cul(COD). Thermochimica Acta, 2007, 456, 89-93.	2.7	15
82	Analysis of silver particles incorporated on TiO2 coatings for the photodecomposition of o-cresol. Thin Solid Films, 2007, 515, 3461-3468.	1.8	93
83	Investigation of thermal stability of Mo thin-films as the buffer layer and various Cu metallization as interconnection materials for thin film transistor–liquid crystal display applications. Thin Solid Films, 2007, 515, 7209-7216.	1.8	37
84	The evolution of diffusion barriers in copper metallization. Jom, 2007, 59, 44-49.	1.9	58
85	A novel two-step MOCVD for producing thin copper films with a mixture of ethyl alcohol and water as the additive. Thin Solid Films, 2006, 498, 43-49.	1.8	15
86	Evaluation of the thermal stability of reactively sputtered (Ti, Zr)Nx nano-thin films as diffusion barriers between Cu and Silicon. Thin Solid Films, 2005, 484, 265-271.	1.8	25
87	Reaction Mechanism of the Two-Step MOCVD of Copper Thin Film Using Cu(hfac)[sub 2]â‹H[sub 2]O Source. Electrochemical and Solid-State Letters, 2005, 8, G307.	2.2	6
88	Diffusion of Copper in Titanium Zirconium Nitride Thin Films. Electrochemical and Solid-State Letters, 2004, 7, C35.	2.2	30
89	Effect of density on the diffusion barrier property of TiNx films between Cu and Si. Materials Chemistry and Physics, 2004, 85, 444-449.	4.0	26
90	Growth of (Ti,Zr)N Films on Si by DC Reactive Sputtering of TiZr in N[sub 2]/Ar Gas Mixtures. Journal of the Electrochemical Society, 2004, 151, C176.	2.9	10

#	Article	IF	CITATIONS
91	Diffusion barrier properties of sputtered TaNx between Cu and Si using TaN as the target. Materials Chemistry and Physics, 2003, 80, 690-695.	4.0	46
92	Characteristics of sputtered TaBx thin films as diffusion barriers between copper and silicon. Applied Surface Science, 2003, 220, 349-358.	6.1	18
93	Characteristics of DC Reactively Sputtered (Ti,Zr)N Thin Films as Diffusion Barriers for Cu Metallization. Electrochemical and Solid-State Letters, 2003, 6, C123.	2.2	8